

Reflection coefficients and optical admittances loci monitoring for thin film coatings and its applications to optical systems

Cheng-Chung Lee*, Kai Wu, and Yu-Jen Chen

Thin Film Technology Center/Department of Optics and Photonics, National Central University,
Chung-Li, Taiwan 320

*cclee@dop.ncu.edu.tw

ABSTRACT

This paper presents an optical monitoring method to find refractive index change and misjudgment of the termination point. This monitoring method is derived from a traditional optical monitor structure. The corresponding error compensations were applied to get good output. Another optical monitoring system is also demonstrated to extract the temporal phase change of the reflection coefficient of the growing film stack. A vibration and air turbulence insensitive polarization interferometers was used in this system to directly detect fluctuating phase and magnitude of the reflection coefficient of a growing film stack as well as the real time optical admittance at normal incidence.

Keywords: Thin film, dynamic interferometer, optical admittance, optical monitor

1. INTRODUCTION

Monitoring is a major factor that influences the performance of the fabrication of optical coatings. Among conventional monitoring methods, time counting monitor or quartz monitor [1] provides thickness controls, but see no refractive index variation or optical performance fluctuation of growing thin films. They cannot do thickness error compensations for previously deposited films in the optical multilayer filter fabrications. Hence, a robust coating machine and an experienced operator are both required in these monitoring procedures, and some filters that are strictly required to have small spectrum error is difficult be fabricated. Since what we concern is the optical performance of film, optical monitoring in which the real time optical performance change can be directly observed is a better way to help operators determine the suitable termination point for each thin film layer during the coating process.

Before running any monitoring process, an initial design satisfying the requirement is necessary to give the operator a guide to control the deposition. One may want the thickness of each deposited thin film layer to be exactly the same as the original design. But in general cases, the refractive indices of materials we input into our coating design are the calculated results from the measurements for one particular chamber, they may vary from time to time under the same environment parameters. Moreover, the refractive index for one layer would fluctuate during the deposition due to the change of the thin film nanostructure. Therefore, in advanced monitoring methods, the refractive index change in one thin film layer should be considered and the corresponding termination point should be revised immediately in order to achieve the best output.

Due to the development of the technology, more complicate design and more strict limitation on the modern coatings are required on various applications, such as laser systems, telecommunication systems, projector systems, and so on. Thus more precise monitoring method is necessary.

In the conventional methods, the most popular one is the variable monochromatic wavelength monitor. Not only does it have more flexibility than single wavelength monitor but also have clearer rule of termination point selection than the broadband wavelength monitor. In broadband monitor [2, 3], there are many wavelengths need to be considered and it is difficult to make sure when is the correct termination time. The transmittance spectrum would not be the same as expected during deposition resulting from the refraction index change or thickness error of the previously deposited films. Although the broadband wavelength monitor can provide more real time inspections of the optical performance of deposited films, they have no clearer mechanism on judging the most important thing in monitor, that is determining the termination point with correct error compensation. Ellipsometry monitor [4] provides the real time information of one

more important factor, phase, and it induces one more parameter, incident angle of light beam, coming from intrinsic property of its work principle. However, it has similar problem as the broadband monitor. Besides, it shall operate with oblique incident angle which makes the system very complicate and costly.

In the conventional monitoring, the termination points are decided according to real time transmittance or reflectance measurement of film stack. Unfortunately, the refractive index and thickness cannot be found as thin film grows, since these two parameters of transmittance or reflectance function are both variable. In other words, the refractive index and thickness are not able to be analytically solved only by transmittance or reflectance measurement at any moment. However, they may be possible to be found from layer to layer by the loci of transmittance or reflectance change during the film deposition. Furthermore, by converting them to the optical admittance loci, the analysis would be easier.

The optical admittance loci or reflection coefficients of film stack growth are broadly used to find revised termination points in monochromatic monitor [5, 6]. Optical admittance provides a clearer way to observe the reflectance change as the film stack thickness changed in different wavelengths. In this article, the monitoring methods by optical admittance and reflection coefficient analysis to improve performance are presented [7, 8]. Moreover, an optical interferometer monitoring system enable to extract reflection coefficient is also demonstrated [9].

2. OPTICAL ADMITTANCE AND REFLECTION COEFFICIENTS ANALYSIS MONITORING FOR THIN FILM DEPOSITIONS

When the thickness of a growing thin film increases, the optical admittance or reflection coefficient under normal incidence follows a circular-like locus on the complex coordinate in the clockwise direction. If the refractive index of the thin film keeps constant during the deposition, the locus of the optical admittance and reflection coefficients will follow an exact circle, as shown in Fig. 1.

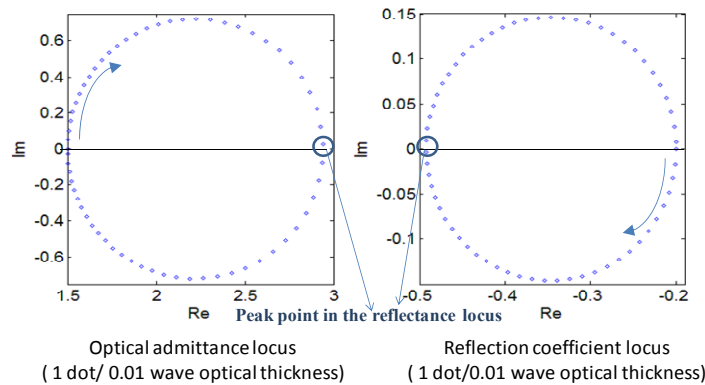


Fig. 1 Optical admittance or reflection coefficient loci ($n_{\text{film}}=2.1, n_{\text{sub}}=1.5$)

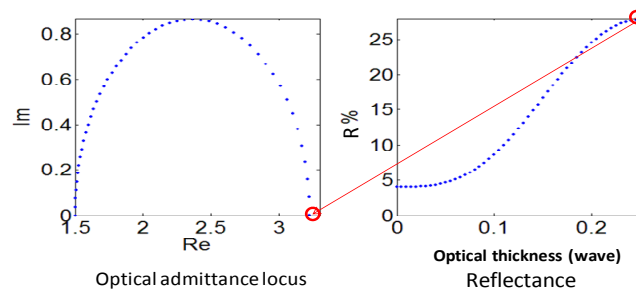


Fig. 2 Reflectance runsheet and optical admittance locus of one layer thin film (1 dot/0.005 wave optical thickness; $n_{\text{film}}=2.1, n_{\text{sub}}=1.5$)

The cross point between loci and real axis, on which the reflection coefficient or optical admittance is a real value, corresponds to the turning points (valley or peak) of the reflectance loci. The reflection coefficient is just equal to $\pm\sqrt{R}$, where R is the reflectance, and the optical admittance is equal to $(1 \mp \sqrt{R})/(1 \pm \sqrt{R})$. Fig. 2 shows simulations of optical admittance loci of one quarter wave thin film layer and its corresponding reflectance locus. One can see that near

the turning point the signal of reflectance changes very slowly as the thickness grows, the sensitivity of the monitor will be very low and it is not easy for an operator to judge the termination point. Thus, the reflectance loci monitor is not good for fabricating the layer of which termination point is near by the turning point.

Among the conventional monitoring methods, Level Monitoring has more sensitive control on thickness than Turning Point Monitoring, but Turning Point Monitoring has better thickness error compensation than Level Monitoring. If the advantages of both can be combined together, the performance would be better. The authors proposed a monitoring method names Selected Sensitive Monitoring Wavelength (SSMW) Method to combine the advantages of both, and their disadvantages can be avoided [7, 8]. Like Level Monitoring, a higher sensitive wavelength was chosen as the monitoring wavelength. Each layer of film stack could have different monitoring wavelength from other layers. The values of turning points were determined from the thicknesses and refractive indices of the deposited thin films. According to this fact, the actual refractive index of the growing film can also be estimated from the turning points.

From the electromagnetic boundary conditions, we can obtain the following equations [10]:

$$\begin{bmatrix} B \\ C \end{bmatrix} = \begin{bmatrix} \cos \delta & \frac{1}{n} \sin \delta \\ \sin \delta & \cos \delta \end{bmatrix} \begin{bmatrix} 1 \\ Y_E \end{bmatrix} \quad \left(\frac{C}{B} = Y \right) \quad (1)$$

where Y_E and Y are the optical admittance of the previously and currently deposited film stack, respectively. n is the refractive index of the currently deposited thin film. δ is the optical phase thickness, which equals to $2\pi nd/\lambda$, d and λ are the physical thickness and measuring wavelength, respectively. The optical admittances of the turning points on reflectance locus were real numbers, as described above. If we develop a thin film characteristic matrix and let the imaginary part of output optical admittance at the turning point be zero, we can write down two equations below:

$$\begin{aligned} \sin \delta \left(\frac{Y_T \alpha}{n} - n \right) - \beta \cos \delta &= 0 \\ \cos \delta (\alpha - Y_T) + \frac{Y_T \beta}{n} \sin \delta &= 0 \end{aligned} \quad (2)$$

where α and β are real and imaginary part of the equivalent optical admittance of Y_E , respectively. $Y_T = (1 \mp \sqrt{R_T}) / (1 \pm \sqrt{R_T})$ is the optical admittance of the turning point, where the sign in front of $\sqrt{R_T}$ depends on the reflection coefficient of the turning point. Thus, the refractive index n can be obtained:

$$n = \frac{\sqrt{(\alpha - Y_T) Y_T (\alpha^2 - Y_T \alpha + \beta^2)}}{\pm (\alpha - Y_T)} \quad (3)$$

Here we should choose the positive root as the proper answer. Then we use this value to predict the proper termination point with error compensation, and the corresponding reflectance can be presented as:

$$R = \frac{((1 - \alpha) \cos \delta' - \frac{\beta}{n} \sin \delta')^2 + ((\frac{\alpha}{n} - n) \sin \delta' - \beta \cos \delta')^2}{((1 + \alpha) \cos \delta' - \frac{\beta}{n} \sin \delta')^2 + ((\frac{\alpha}{n} + n) \sin \delta' + \beta \cos \delta')^2} \quad (4)$$

where δ' is the optical phase thickness for the current layer. Since the refractive index has been known from Eq. (3), we can obtain the exact grown thickness with the termination reflectance value by solving Eq. (4). Following the procedures described above, we can monitor the thickness and refractive index of deposited films more precisely. The corresponding errors can be compensated by terminate the deposition on the new cross point with the expected admittance locus of next layer. Let the locus go back to the originally expected locus, and the final optical admittance in the design could be reached in the monitoring wavelengths, as well as other nearby wavelengths.

In narrow-band pass filter production, the proper thickness with error compensation should no longer be a quarter-wave due to the error of previous layers. Since the refractive index and thickness of each layer has been found, the equivalent optical admittance of film stack could be found when the deposition of one layer is complete. The compensation thickness will make the admittance of the end point for central wavelength to be a real number (imaginary part is zero). Convert the obtained refractive indices and optical thickness to those of the central wavelength and its corresponding phase thickness should be [8]:

$$\delta_c = \tan^{-1} \left(\frac{1}{2\beta_c n_c} (n_c^2 - \beta_c^2 - \alpha_c^2 \pm (n_c^4 + 2\beta_c^2 n_c^2 - 2n_c^2 \alpha_c^2 + \beta_c^4 + 2\beta_c^2 \alpha_c^2 + \alpha_c^4)^{1/2}) \right) \quad (5)$$

where n_c is the refractive index for central wavelength. α_c and β_c are the real and imaginary part of the equivalent admittance at the current layer's beginning point for the central wavelength, respectively.

Convert it back to the corresponding thickness for a sensitive monitoring wavelength, the corresponding termination point on transmittance (or reflectance) runsheet then can be calculated. It will keep the spectrum of final output at correct position, even though the sensitive wavelength instead of central wavelength is selected to be the monitoring wavelength. Figure 3 shows the experimental results. One can see that SSMW method has much better error compensation than Level Monitor Method, and it also has narrower bandwidth than the Turning Point Method.

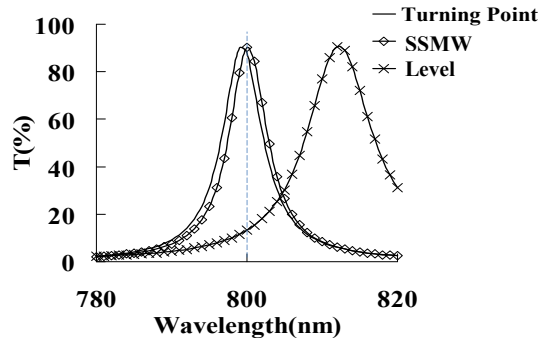


Fig. 3 SSMW method experimental results comparing with other conventional methods ((HL)4H 2L H(LH)4 Structure; central wavelength: 800nm) [8]

3. REAL TIME PHASE OF REFLECTION COEFFICIENTS MONITORING SYSTEM FOR THIN FILM DEPOSITIONS

However, the refractive indices may gradually change from time to time, and the optical admittance locus would slightly shift. The corresponding calculation errors derived from this assumption would be accumulated as layer number increase. The real time refractive index variation could be observed only in a monitor system from which the optical phase of a growing film stack can be extracted, like an ellipsometry monitor. But using the ellipsometry monitor we cannot obtain the reflection coefficient at normal incidence due to the working principle and needs numerical algorithm fitting to guess the real answers. A monitor system for extracting the real-time reflection phase and magnitude of monitoring light coming from a growing thin film stack was proposed for solving this problem and achieving the finer monitor. A dynamic polarization interferometer will be applied in the system to erase the mechanical vibration and air turbulence and obtain the reflection coefficient, optical admittance, refractive index and thickness at every moment. It provides a powerful and global monitoring for coatings. An interferometer using temporal phase-shifting is very sensitive to vibration because the various phase shifted frames of interferometric data are taken at different times and vibration causes the phase shifts between the data frames to be different from what is desired. Vibration effects can be reduced by taking all the phase shifted frames simultaneously [11-13].

A Fizeau polarization interferometer utilizing a micropolarize phase-shifting array is used to extract the optical phase, as shown in Fig. 4. The interferometers applied to measure the phase instantaneously and that we use it to track one phase signal in real time. The two quarter-wave plates placed around the polarization beam splitter (PBS) were oriented to convert S to P polarized beam reflected from one mirror and P to S polarized reflected from the other mirror, respectively. The polarization Twyman-Green interferometer was employed to eliminate the optical path difference between test and reference beams so that the corresponding interference fringes can be observed under low coherence light source. In our case, test surface locates at the side where the thin film grows, and the other side of substrate is the reference surface, so the optical path difference between test and reference beams is just double optical thickness of the substrate. Since what our concern is the change coming from the thin film growth instead of the whole surface profile, we only need to focus on one point of the sample just as the traditional coating monitor and do not care too much about the flatness of the reference surface.

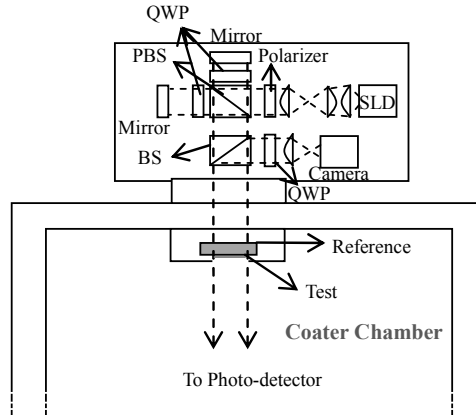


Fig. 4 Optical interferometry monitor system layout

The reflections in the Fizeau cavity, that is the substrate, can be illustrated as Fig. 5. The rays are drawn spatially separate and with a slight slant in the sketch, but are all normal to the surface and collinear in the monitoring system. The numbers within the cavity indicate the number of test surface reflections of each beam has passed before it exited the cavity. If we make the length difference between the two arms of the Twyman-Green interferometer is almost equal to twice of the optical thickness of the substrate, only the paired beams that are path matched and drawn in the same type of lines will interfere with each other at the polarizers on the camera due to short coherence length of light. Each successive reflection of the s-polarized beam off of the test surface is coherent with the p-polarized beam that has undergone one additional test surface reflection. The matched paths S_0 and P_1 , and S_1 and P_2 , etc. are drawn with the same type of lines (e.g. dashed line for S_0 and P_1 , dotted line for S_1 and P_2). The quarter-wave plat in front of the camera is oriented to convert two polarized beams coming from two arms of interferometer into two orthogonally circular polarization states. The detecting element is a micro-polarizer pixelated camera, and the adjacent pixels have different orientation polarizer on them. Upon passing through the polarizer at an angle α , it will generate a phase sifting of 2α between the two orthogonally polarized light beams. The light intensity at detector will be [13]:

$$I = I_1 + I_2 + 2\sqrt{I_1 I_2} \cos(\varphi + 2\alpha) \quad (6)$$

The linear polarizer acts as a phase shifting device between the two beams, were the phase shift, 2α , is equal to twice the orientation angle of the polarizer. The detecting element in the system is a micro-polarizer pixelated camera, and the adjacent pixels have different orientation polarizer on them as shown in Fig. 6. The measured intensity can be presented as:

$$\begin{aligned} I_{\text{measured}} &= I_{P_0} + I_{S_0} + 2\sqrt{I_{S_0} I_{P_1}} \cos(\varphi + 2\alpha) + I_{P_2} + I_{S_1} + 2\sqrt{I_{S_1} I_{P_2}} \cos(\varphi + 2\alpha) + \dots + I_{P_n} + I_{S_{n-1}} + 2\sqrt{I_{P_n} I_{S_{n-1}}} \cos(\varphi + 2\alpha) \\ &= (I_S + I_P) \left(R_r + \frac{(1 - R_r)^2 R_t}{1 - R_r R_t} \right) + 2(1 - R_r) \sqrt{I_S I_P} \sqrt{R_r R_t} \left(\frac{(1 - R_r)}{1 - R_r R_t} \right) \cos(\varphi + 2\alpha) = I_{DC} + I_{AC} \cos(\varphi + 2\alpha) \end{aligned} \quad (7)$$

where R_r and R_t are the reflectance from the reference and test surfaces, respectively. $\varphi = \delta_{\text{film}} + \Gamma - 2D$ is the phase difference between the two beams in each interfering beam pair, where the phase of the thin film reflection coefficient is δ_{film} , D is the optical thickness of substrate, and Γ is the phase difference of S and P polarization.

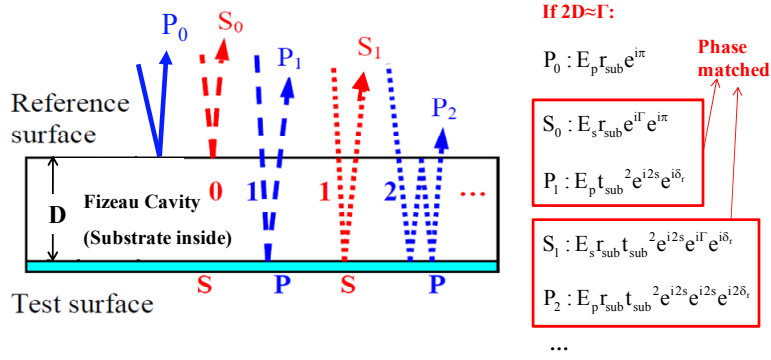


Fig. 5 Reflections in the substrate

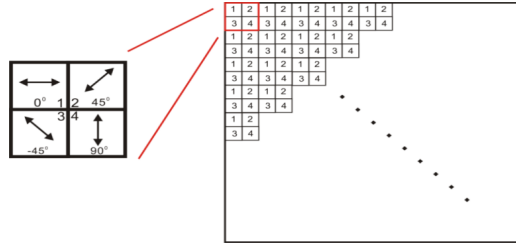


Fig. 6 Micropolarizer distribution on camera

Four different polarizers at 0° , 45° , -45° , 90° , respectively, on the camera, generate four different phase shifted interferograms simultaneously. Therefore, each pixel can generate different phase shift to the adjacent pixels for phase shifting algorithm. The reflection phase of growing films coming from the test surface can be acquired by the phase-shifting algorithm in a single camera frame to freeze vibration effect:

$$\varphi = \tan^{-1} \left[\frac{2(I_2 + I_8 - I_4 - I_6)}{(-I_1 - I_3 + 4I_5 - I_7 - I_9)} \right] \quad (8)$$

There is a photo-detector placed under the coater to measure transmittance, T . Then the reflectance, R , can be calculated by $1-T$. The magnitude of the reflection coefficient, square root of R thus can be further acquired. After reflectance magnitude and phase are acquired, the reflection coefficient at normal incidence of light is known and optical admittance can be calculated by following relation:

$$\frac{n_s - (\alpha + i\beta)}{n_s + (\alpha + i\beta)} = |r_{\text{film}}| e^{i\delta_{\text{film}}} \quad (9)$$

where r_{film} is magnitude of the reflection coefficient, and n_s is the refractive index of the incident medium. In our case, the incident medium is substrate. α and β are given by follows.

$$\alpha = \frac{n_s (1 - |r_{\text{film}}|^2)}{1 + |r_{\text{film}}|^2 + 2|r_{\text{film}}| \cos \delta_{\text{film}}}, \quad \beta = \frac{-2n_s |r_{\text{film}}| \sin \delta_{\text{film}}}{1 + |r_{\text{film}}|^2 + 2|r_{\text{film}}| \cos \delta_{\text{film}}} \quad (10)$$

For non-absorption films, refractive index and thickness variation at every moment can also be calculated. According to Eq. (1), the optical admittance can be written down as:

$$\alpha + i\beta = \frac{in \sin \delta + (\alpha' + i\beta') \cos \delta}{\cos \delta + \frac{i\alpha' - \beta'}{n} \sin \delta} \quad (11)$$

where $\alpha' + i\beta'$ and $\alpha + i\beta$ are the admittance of the previously deposited film stack and the new equivalent admittance, respectively. δ is the optical phase thickness of newly deposited thin film, n is the corresponding refractive index. The solutions of Eq. (11) are:

$$n = \pm \frac{\sqrt{(\alpha - \alpha')(\alpha^2 \alpha' - \alpha \alpha'^2 + \alpha' \beta^2 - \alpha \beta'^2)}}{(\alpha - \alpha')} \quad \delta = \arctan\left[\pm \left(\frac{\sqrt{(\alpha - \alpha')(\alpha^2 \alpha' - \alpha \alpha'^2 + \alpha' \beta^2 - \alpha \beta'^2)}}{\alpha' \beta + \alpha \beta'}\right)\right] \quad (12)$$

We should always choose the set of answer whose n and δ are positive. Thus, the complete information about reflection coefficient, optical admittance, refractive index and actual thickness of the growing film stack at every moment can be observed through this optical monitor system. Unlike other optical admittance monitor, the calculation error would not accumulate in this system, because the calculation is not relative to previous calculations.

Before the deposition, the phase difference between the reference area and the monitored area was 2.2787. (Average 30 pixels data) The phase difference between the reference area and the monitored area after the deposition was 0.1675. Hence, the optical phase resulted from the thin films was -2.1112 (radians). The measured reflectance of Ta₂O₅ thin film was 16.21%. Table 1 shows the calculated results from the monitor system and ellipsometer measurement.

Table 1 Comparison between the results by monitor system and ellipsometer measurements

	Refractive index	Thickness	Reflection coefficient	Optical admittance
Monitor system measurement	2.119	39.039nm	-0.20708 - 0.34514i	1.6405 + 1.3513i
Ellipsometer measurement	2.168	39.04nm	-0.23321 - 0.35071i	1.6939 + 1.4443i

The experimental result is very close to the ellipsometer measurement fitting results. But unlike ellipsometer, the phases were directly grabbed from the normal incident light. The experimental results satisfied what we expected.

4. CONCLUSIONS

A method to estimate the fluctuation of the refractive index during thin film deposition through optical admittance analysis was described in this article. The thicknesses and error-compensated thickness for each layer are analyzed. The revised refractive index and the choice of highly sensitive monitoring wavelengths help us to predict the termination points more accurately. The experimental results demonstrate that it has superior performance. Furthermore, a monitor system for the extraction of both intensity and phase was also presented. It is an optical interferometry system with high vibration insensitive. Through this system the reflection coefficient, optical admittance, refractive index, and actual thickness can be analytically calculated at every moment for the growing film stack. It would be a powerful monitor system for optical thin film deposition. Combining with high sensitive monitor of optical admittance, it would improve the performance of optical monitor and be useful in the fabrication of valuable coating elements, such as filters in laser systems, telecommunication systems, projector systems, and so on.

ACKNOWLEDGEMENT

The authors would like to thank 4D Technology for offer pixelated micro-polarizer camera and technical guidance of interferometer construction and the National Science Council of Taiwan for providing financial support under project NSC 099-2221-E-008-046-MY3.

REFERENCES

- [1] A. Wajid, "On the accuracy of the quartz-crystal microbalance (QCM) in thin-film depositions," *Sensors and Actuators A* 63, 41 (1997)
- [2] B. Badoil, F. Lemarchand,* M. Cathelinaud, and M. Lequime" Interest of broadband optical monitoring for thin-film filter manufacturing", *Appl. Opt.* 46, 4294 (2007)
- [3] S. Wilbrandt, N. Kaiser *, O. Stenzel "In-situ broadband monitoring of heterogeneous optical coatings," *Thin Solid Films* 502, 153 (2005)
- [4] S. Dligatch, R. Netterfield, and B. Martin, "Application of in-situ ellipsometry to the fabrication of multilayered coatings with sub-nanometre accuracy," *Thin Solid Films* 455-456, 376 (2004)

- [5] C.C. Lee and Y.J. Chen, "Multilayer coatings monitoring using admittance diagram," *Opt. Exp.* 16, 6119 (2008)
- [6] B. Chun, C. K. Hwangbo, and J. S. Kim, "Optical monitoring of nonquarterwave layers of dielectric multilayer filters using optical admittance," *Opt. Express* 14, 2473 (2006)
- [7] C.C. Lee, K. Wu, C.C. Kuo and S.H. Chen, "Improvement of the optical coating process by cutting layers with sensitive monitor wavelengths", *Optics Express* 13, 4854 (2004)
- [8] C. C. Lee and K. Wu, "In situ sensitive optical monitoring with proper error compensation", *Optics Letters*, 32, 2118 (2007)
- [9] C. C. Lee, K. Wu, S. H. Chen , and S.R. Ma "Optical monitoring and real time admittance loci calculation through polarization interferometer," *Optics Express*, 15, 7536 (2007)
- [10] H. A. Macleod, [*Thin Film Optical Filters*], 3rd ed, Inst. of Physics Publishing, (2001).
- [11] B. Kimbrough, J. Millerd, J. Wyant, J. Hayes, "Low Coherence Vibration Insensitive Fizeau Interferometer," *Proc. SPIE* 6292, 62920F (2006).
- [12] N. Brock, J. Hayes, B. Kimbrough, J. Millerd, M. North-Morris, M. Novak and J. C. Wyant, " Dynamic interferometry ," *Proc. SPIE* 5875 , 58750F (2005).
- [13] J. Millerd, N. Brock, J. Hayes, B. Kimbrough, M. Novak, M. North-Morris and J. C. Wyant, "Modern Approaches in Phase Measuring Metrology ," *Proc. of SPIE* 5856, 14 (2005)